

Effects of Limiting Matrix Diffusion of Radionuclide in Fractured Porous Rock : Back Diffusion of Np-237

Jin Beak Park, Youngsoo Hwang and Chul Hyung Kang
Korea Atomic Energy Research Institute
150 Dekjin-Dong, Yousong-Gu
Taejon 305-353 Korea

ABSTRACT

In a previous paper, the authors have presented the effect of the limiting zone for the matrix diffusion of I-129 from an open fracture into a surrounding porous medium to reflect recent field findings from field studies. In addition to this matrix diffusion into finite porous rock matrix, this study analyzes the back diffusion of Np-237 from finite rock matrix into a fracture with band release condition. When the finite thickness of rock matrix is considered with band release, Np-237 are transported further along the fracture and the radionuclides stored during leaching time in surrounding rock matrix diffuse back into the fracture rapidly making peak diffusive flux.

1. Introduction

Fractures have been considered as the primary pathway of groundwater flow and consequent radionuclide transport in the long-term performance assessment of a deep geologic repository in crystalline rocks such as granite.

Authors [1] presented, in a previous paper, the effect of limiting matrix diffusion from a fracture into a porous rock by numerical inversion of the Laplace transform to reflect the result of recent field findings [2-7]. These field studies have challenged the traditional concept of matrix diffusion into a surrounding rock. Natural analogues and laboratory experiments [2-4] showed pore connectivity over several tens of centimeters in the rock matrix. The penetration may, however, be limited by sorption and by the lower diffusivity in the unaltered rock matrix further away from the water-conducting fracture.

According to a fracture-mapping study of granodiorite [5], fractures can be classified into three types: type A with a zone of fracture fillings, type B with both a zone of fracture fillings and an altered zone, and type C consisting of several fractures with a zone of fracture fillings and an altered zone. Among the fracture types, the fracture type B was predominant and typical in the studies area with 60% of the fractures observed. Since the fracture type A is included in the fracture type B, judging from the fracture structure and mineralogy, the fracture type B after all occupies 99% of the studied area. Sato [6] reported the pore properties of fracture type B that the average porosity was 0.056 for fracture fillings, 0.032 for altered granodiorite, and 0.023 for intact granodiorite. The effective diffusion coefficient value was reported as 0.49 to 2.8×10^{-11} m²/s for fracture fillings, 0.24 to 2.5

$\times 10^{-11}$ m²/s for altered granodiorite, and 0.072 to 1.7×10^{-11} m²/s for intact granodiorite. In the numerical model [7], the maximum penetration depth of matrix diffusion is limited to 10 cm due to computational reasons.

In addition to matrix diffusion into finite porous rock matrix, this study analyzes the back diffusion of Np-237 from finite rock matrix into a fracture with band release condition. Back diffusion is explained by normalized diffusive flux of Np-237 at the interface of a fracture and surrounding rock matrix depicted in Fig. 1.

Analytic solution of this transport system was derived earlier by the author [8]. In this paper, to avoid the numerical difficulties of multiple integration that mainly come from the highly oscillatory integrand, numerical inversion of the Laplace transform is employed to evaluate the radionuclide concentration in water both in a fracture and in a porous rock matrix. The package subroutine DINLAP of IMSL Library [9] is used to perform numerical inversion of the Laplace transform with relative accuracy of 10^{-6} .

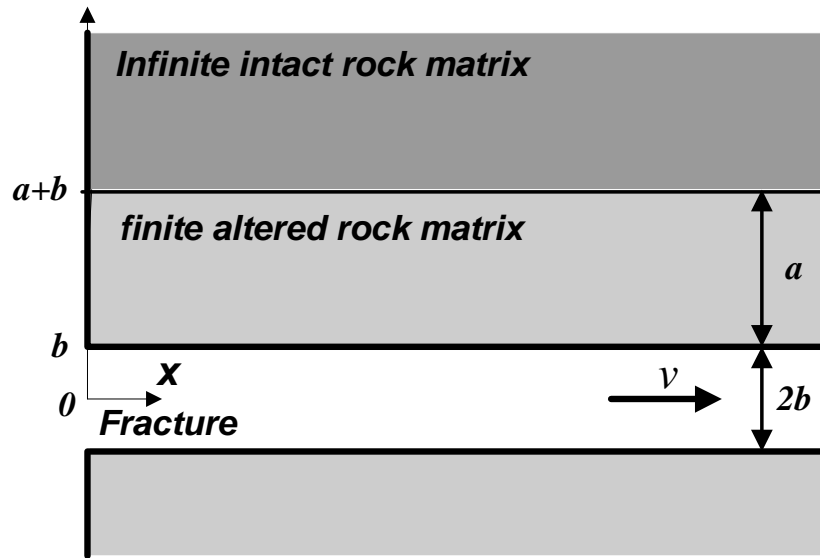


Figure 1 Physical system for the limiting matrix diffusion from a single, planar fracture into a finite rock matrix with a thickness a

2. Mathematical Formulation

The real physical system is idealized as shown in Fig. 1. The fracture is modeled as a planar one with an aperture of $2b$. The surrounding rock is simplified as a water-saturated porous medium with an effective porosity of θ . The transport mechanisms in the fracture are advective transport along the fracture, longitudinal hydrodynamic dispersion in the fracture in the direction of the fracture axis, and molecular diffusion into the rock matrix. Inside the rock, only the matrix diffusion is considered because the permeability is low. In addition, sorption onto the interface of the fracture and the surrounding medium, rather strong sorption in the rock matrix and radioactive decay with no precursor are considered.

The fracture aperture is much smaller than the fracture length so that after a certain distance from the fracture inlet, the flow is fully developed. In that sense, it is reasonable to take the pore water velocity, v , as constant.

Also, if aperture is so thin, the flow is assumed well mixed across the fracture so that the y dependency inside the fracture can be ignored in mathematical modeling.

From the mass balance theory with the above assumptions, the governing equation for transport of a radionuclide in the fracture [10] is derived as:

$$R_f \frac{\partial N(x,t)}{\partial t} - D_f \frac{\partial^2 N(x,t)}{\partial x^2} + v \frac{\partial N(x,t)}{\partial x} + R_f \lambda N(x,t) + \frac{q}{b} = 0, x > 0, t > 0, \quad (1)$$

$N(x,t)$ = concentration of the radionuclide in fracture water [kg-nuclide/m³-water],

R_f = retardation coefficient on the fracture matrix interface, [-], defined as:

$$R_f = 1 + K_f / b, \quad (2)$$

K_f = surface distribution coefficient of a radionuclide per unit area of the fracture rock interface over the unit volume [m],

b = fracture half width [m],

D_f = longitudinal dispersion coefficient [m²/yr],

λ = radioactive decay constant [1/yr],

x = distance from a fracture inlet along the fracture [m],

t = time since the release of a radionuclide at the inlet [yr],

$q(x,t)$ = diffusive flux of a radionuclide from the fracture into the rock matrix [kg-nuclide/m² yr] defined as:

$$q(x,t) = -\theta D_p \left. \frac{\partial M(x,y,t)}{\partial y} \right|_{y=b}, x > 0, t > 0, \quad (3)$$

θ = porosity of the surrounding rock matrix [-],

$M(x,y,t)$ = concentration of the radionuclide in rock matrix water [kg-nuclide/m³-water],

D_p = pore diffusion coefficient in a rock matrix [m²/yr],

y = distance from a centerline of the fracture [m].

Similarly, the governing equation describing the movement of a radionuclide in the rock matrix is:

$$R_p \frac{\partial M}{\partial t} - D_p \frac{\partial^2 M}{\partial y^2} + R_p \lambda M = 0, x > 0, b < |y| < a + b, t > 0, \quad (4)$$

R_p = retardation coefficient in the rock matrix [-], defined as:

$$R_p = 1 + \frac{(1-\theta)}{\theta} \rho_p K_p, \quad (5)$$

K_p = distribution coefficient in the rock matrix [m³/kg],

ρ_p = density of the rock matrix [kg/m³].

Side conditions of Eq. (1) and Eq. (4) are

$$N(x,0) = 0, x > 0, \quad (6)$$

$$M(x,y,0) = 0, x > 0, b < |y| < a + b, \quad (7)$$

$$N(0,t) = N_0 e^{-\lambda t}, t > 0, \quad (8)$$

$$N(\infty,t) = 0, t > 0, \quad (9)$$

$$M(x,b,t) = N(x,t), x > 0, t > 0, \quad (10)$$

$$\partial M(x, y, t) / \partial y \Big|_{y=a+b} = 0, x > 0, t > 0. \quad (11)$$

where N_o is the source concentration at the fracture inlet.

Eqs. (6) and (7) indicate zero initial conditions. Eq. (8) describes the decaying inlet boundary condition and Eq. (9) depicts the zero boundary condition at the outlet. Eq. (10) explains the concentration continuity at the fracture and rock interface. The remaining boundary condition, Eq. (11) is the key of the problem. It stipulates the limiting capacitance of the matrix diffusion at a meter into the rock from the fracture and matrix interface. Beyond this point, the rock is practically impermeable so that no nuclides can penetrate into any further.

Eqs. (1) and (4), subject to their initial and boundary conditions, can be solved by applying the Laplace transform with respect to t . Applying the Laplace transform of Eq. (4) with the initial condition, Eq. (7), the following equation is derived as:

$$\frac{d^2 \tilde{M}}{dy^2} - \frac{R_p}{D_p} (p + \lambda) \tilde{M} = 0, b < |y| < a + b, \quad (12)$$

where the tilde symbol \sim stands for the Laplace-transformed variable and p is the Laplace variable in a complex domain. Eq. (12) is solved with the Laplace-transformed boundary conditions as:

$$\tilde{M}(x, b, p) = \tilde{N}(x, p), x > 0, \quad (13)$$

and

$$d\tilde{M}(x, y, p) / dy \Big|_{y=a+b} = 0, x > 0. \quad (14)$$

The solution of Eq. (12) can be written as:

$$\tilde{M}(x, y, p) = \tilde{N}(x, p) \frac{\cosh(B\sqrt{p + \lambda}(y - a - b))}{\cosh(aB\sqrt{p + \lambda})}, x > 0, b \leq |y| \leq a + b, \quad (15)$$

where

$$B = \sqrt{R_p / D_p}. \quad (16)$$

The Laplace-transformed diffusive flux across the rock-fracture interface, \tilde{q} , can be obtained from the following:

$$\tilde{q}(x, p) = -\theta D_p d\tilde{M} / dy \Big|_{y=b} = \theta D_p B \sqrt{p + \lambda} \tanh(aB\sqrt{p + \lambda}) \tilde{N}. \quad (17)$$

Applying the Laplace transform to Eq. (1) with the initial condition of Eq. (6) and substituting Eq. (17) into the resultant equation yields:

$$\frac{d^2 \tilde{N}}{dx^2} - \frac{v}{D_f} \frac{d\tilde{N}}{dx} - \frac{R_f}{D_f} \left\{ (p + \lambda) + \alpha \sqrt{p + \lambda} \tanh(aB\sqrt{p + \lambda}) \right\} \tilde{N} = 0, x > 0, D_f \neq 0, \quad (18)$$

where

$$\alpha = \theta \sqrt{R_p D_p} / b R_f. \quad (19)$$

Eq. (18) can be solved with the following Laplace transformed boundary conditions as:

$$\tilde{N}(0, p) = N_o / (p + \lambda), \quad (20)$$

and

$$\tilde{N}(\infty, p) = 0. \quad (21)$$

The final Laplace transformed normalized solution of $N(x, t)$ is depicted as:

$$\frac{\tilde{N}(x, p)}{N_o} = \frac{e^{\beta x}}{p + \lambda} \exp[-x \sqrt{\beta^2 + \gamma [p + \lambda + \alpha \sqrt{p + \lambda} \tanh(aB \sqrt{p + \lambda})]}], x \geq 0, D_f \neq 0, \quad (22)$$

where

$$\beta = v/2D_f \text{ and } \gamma = R_f / D_f. \quad (23) \text{ and } (24)$$

If a band release mode is considered, Eq. (8) is rewritten as:

$$N(0, t) = N_o e^{-\lambda t} [h(t) - h(t - T)], t > 0, \quad (25)$$

where T is the leach time. The superposition technique [11] can be used to find the general solution after the numerical inversion of Laplace transform, which is subject to Eq. (27) as:

$$N^b(x, t) = N(x, t)h(t) - e^{-\lambda T} N(x, t - T)h(t - T), \quad (26)$$

and

$$M^b(x, y, t) = M(x, y, t)h(t) - e^{-\lambda T} M(x, y, t - T)h(t - T), \quad (27)$$

where superscript b indicates the band release solution.

3. Numerical Evaluations

Based on the input data presented in Table 1, Fig. 2 shows the profile of $N(x, t)/N_o$ after the end of leach time at 50,000 yr considering band type release of Eq. (26). As the altered thickness, a , increased to 50 m, normalized concentration for the case of finite rock matrix approaches to that for the case of infinite rock matrix.

Fig. 3 shows the normalized concentration of $N(x, t)$ as a function of distance along the fracture between the infinite rock matrix and the finite rock matrix of 1 m thickness at times 10,000 yr and 50,000 yr. Solid lines stand for the case of finite rock matrix and dotted lines for the case of infinite rock matrix.

In Fig. 3, it is evident that radionuclides are accelerated in water in the fracture before the end of leach time ($t = 10\ 000$ yr). After the end of leach time ($t = 50\ 000$ yr), the location of peak concentration moves further and the peak value shows higher value in case of finite rock matrix.

Table 1 Input parameters for the numerical evaluations

Species		²³⁷ Np			
D_f	(m ² /yr)	1	v	(m/yr)	1.0
D_p	(m ² /yr)	0.01	$T_{1/2}$	(yr)	2.14×10^6
R_f	(-)	1	b	(m)	5.0×10^{-4}
R_p	(-)	10	θ	(-)	0.01
a	(m)	0.1, 0.5, 1.0 ⁽¹⁾ , 5.0, 10.0, 50.0	T	(yr)	30 000

(1) Reference value

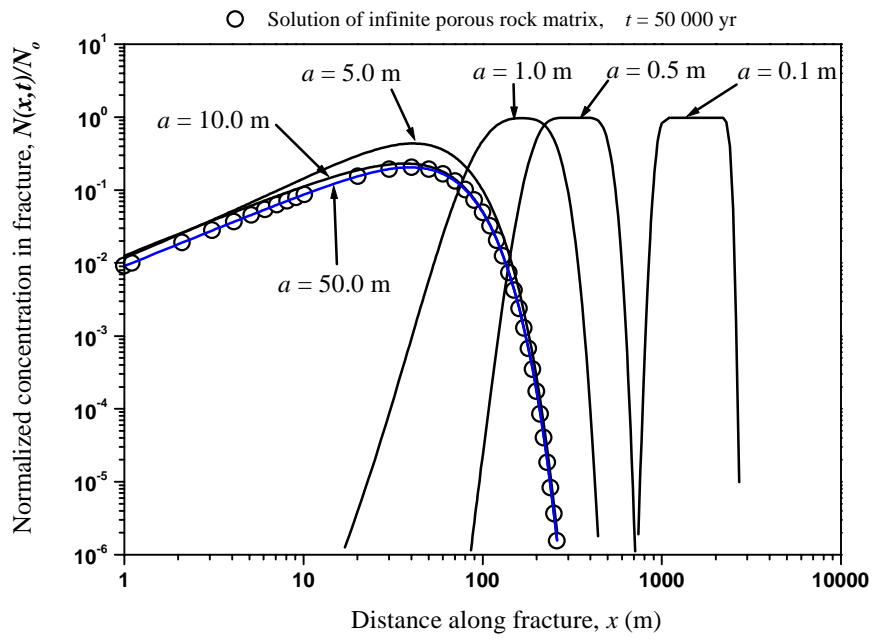


Figure 2 Normalized concentration of $N(x,t)$ with different thickness of finite altered rock matrix, $t = 50,000$ yr

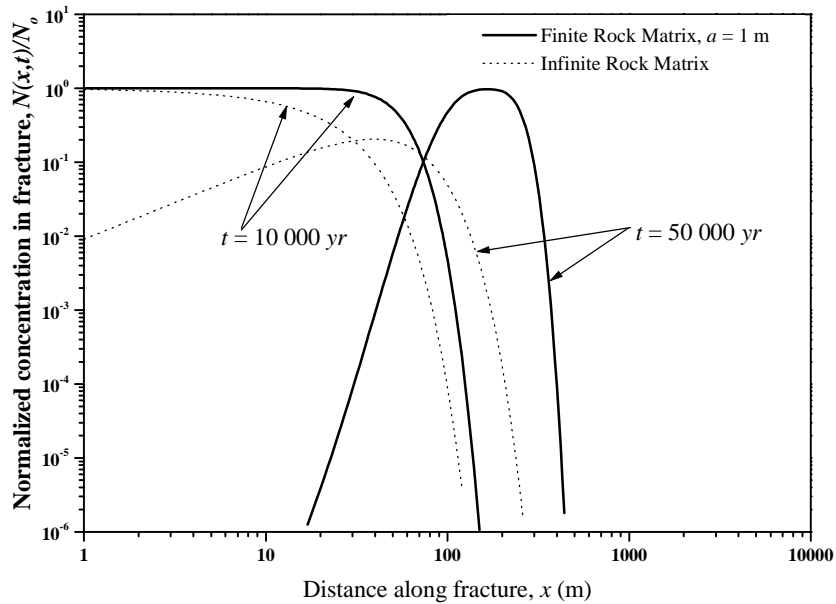


Figure 3 Normalized concentration of $N(x,t)$ as a function of distance along the fracture between the infinite and the finite rock matrix ($a=1$ m), $t = 10\,000$ yr and $50\,000$ yr

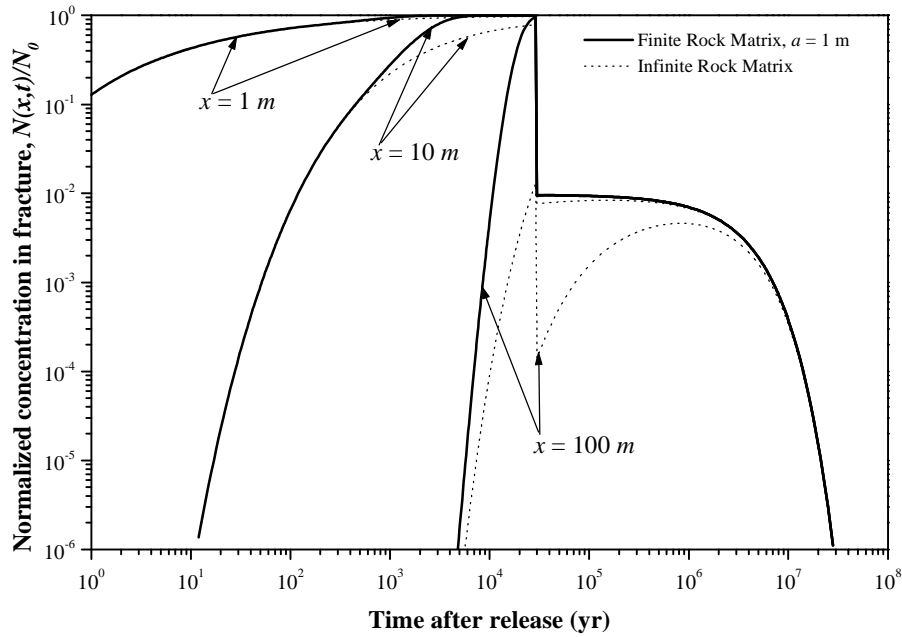


Figure 4 Normalized concentration of $N(x,t)$ as a function of time after release at three different location between the infinite and the finite rock matrix ($a = 1\text{m}$)

Fig. 4 shows normalized concentration of $N(x,t)$ as a function of time after release at different locations along the fracture. Higher concentrations of solid line in the fracture before the leach time ($t < T$) mean accelerated transport of radionuclide in the finite rock system. Higher concentrations of solid line just after the leach time ($t > T$) mean that more radionuclides diffuse back from rock matrix into the fracture than in the case of the transport system with infinite rock matrix.

In Fig. 5, diffusive fluxes normalized by the initial concentration at the boundary are plotted against the distance along the fracture axis. When the system with infinite rock matrix and that with finite rock matrix are compared, apparently different flux profiles are obtained.

In Fig. 5 (a), diffusive fluxes near the fracture inlet at the end of leach time ($t = T$) show 10^{-5} [$\text{kg}/\text{m}^2 \text{ yr}$] in case of infinite rock matrix and 10^{-12} [$\text{kg}/\text{m}^2 \text{ yr}$] in case of finite rock matrix ($a = 1 \text{ m}$). This means that the saturation of finite rock matrix is reached earlier than of infinite rock matrix due to limited amount of radionuclide storage and, thus, radionuclides are transported rapidly by advection and hydrodynamic dispersion in the fracture for the finite rock matrix. It is found that, in case of system with finite rock matrix, the position of the maximum diffusive flux moves away from the fracture inlet as shown in Fig. 5 (a). Whereas, in case of system with infinite rock matrix, diffusive flux profiles along the fracture axis are maintained as far as the concentration front in a fracture is reached and apparent position representing the maximum diffusive flux does not appear.

After the end of leach time ($t > T$), it is evident that the back diffusion from the porous rock matrix to the fracture occurs in Fig. 5 (b). Negative diffusive fluxes, which follow foregoing positive flux, represent this back

diffusion. This means that surrounding rock matrix of finite or infinite extend plays a role as the radionuclide storage buffer during the leach time, T . Higher peak flux and further peak location for the case of finite rock matrix, in Fig. 5 (b), is due to the limited amount of storage capacity of the surrounding finite rock matrix.

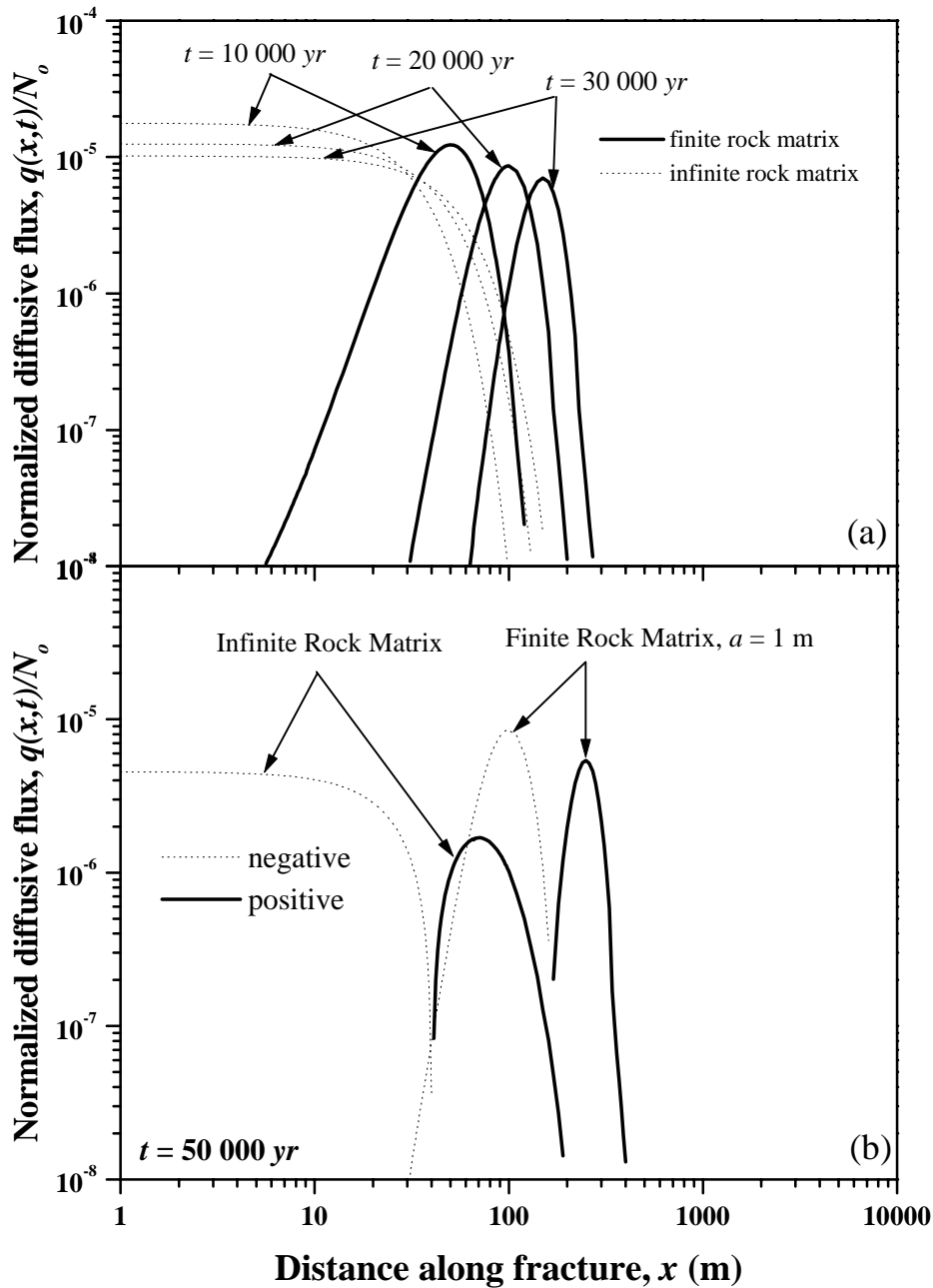


Figure 5 Normalized diffusive mass flux across the rock-fracture interface, Negative fluxes in the figure (b) mean that radionuclides diffuse back from rock matrix to a fracture.

4. Conclusions

A recent field survey indicated that a portion of the surrounding rock matrix is available for matrix diffusion of radionuclides from a fracture. If this observation is true, then the current matrix diffusion models allowing diffusion into an infinitely long matrix certainly overemphasize the potential retardation caused by the matrix diffusion. Therefore, to judge whether the current conceptual models for performance assessment are still conservative or not, new mathematical modeling is needed to reflect the recent field results.

The results indicate that, for smaller thickness of permeable rock matrix, normalized concentrations deviate from those by the solution without the impermeable zone. However, for large thickness of permeable rock matrix the two cases are almost identical. When the finite thickness of rock matrix is considered with band release, Np-237 are transported further in the fracture and the stored Np-237 during leach time in surrounding rock matrix diffuses back into the fracture rapidly making peak diffusive flux. Therefore, for conservative performance assessment, this model would be suitable in case of small thickness of permeable rock matrix with low fracture density.

5. References

1. Park, J.B., Lee, K.J., and Hwang, Y. (2001), "Effects of Limiting Matrix Diffusion of Radionuclide in Fractured Porous Rock : Numerical Inversion of Laplace Transform," *Proceedings of the Korean Nuclear Society Spring Meeting*, Cheju.
2. Ohlsson, Y. and Neretnieks, I. (1995), *Literature survey of matrix diffusion theory and of experiments and data including natural analogues*, Technical Report 95-12, SKB, Stockholm.
3. Hartikainen, J., *et al.* (1996), *Helium gas methods for rock characteristics and matrix diffusion*, POSIVA 96-22,, Helsinki.
4. Rasilainen, K. (1997), *Matrix diffusion model - In situ tests using natural analogues*, VTT Publications 331, Technical Research Centre of Finland, Espoo.
5. Osawa, H., *et al.* (1994), "Development of a conceptual flow-path model of nuclide migration in crystalline rock - A case study at the Kamaishi in-situ test site, Japan," *Proc. 18th Symp. Scientific Basis for Nuclear Waste Management*, Kyoto, Japan, Oct. 23-27, 1267.
6. Sato, H. (1999), "Matrix Diffusion of Simple Cation, Anion and Neutral Species in Fractured Crystalline Rocks", *Nuclear Technology*, Vol.127, pp. 199-211.
7. Vieno, T. and Nordman, H. (1999), *Safety Assessment of spent fuel disposal in Hastholmen, Kivetty, Olkiluoto and Romuvaara TILA-99*, POSIVA 99-07, POSIVA, Helsinki.
8. Park, J.B., Hwang, Y., and Lee, K.J. (2001), "Analytic Solutions of Radionuclide Transport with the Limited Diffusion from the Fracture into a Porous Rock Matrix," *Annals of Nuclear Energy*, Vol.28, No.10, pp. 993-1011.
9. Numerics, V. (1997), *IMSL Fortran subroutines for Mathematical Applications*.
10. Ahn, J. (1988), *Mass Transfer and Transport of Radionuclides in Fractured Porous Rock*, Ph. D. Dissertation, Univ. of California at Berkeley.

11. Harada, M., *et al.* (1980), *Migration of Radionuclides through sorbing media: Analytical solution - I*, LBL-10500, Lawrence Berkeley Laboratory, Berkeley.